COMMUNICATION

OBC
www.rsc.org/obc

Rational design of new bifunctional inhibitors of type II dehydroquinase†

Miguel D. Toscano,[a] Kirsty A. Stewart,[b] John R. Coggins,[c] Adrian J. Lapthorn[b] and Chris Abell*[a]

[a] *University Chemical Laboratory, Lensfield Road, Cambridge, UK CB2 1EW. E-mail: ca26@cam.ac.uk; Fax: 44 1223 336362; Tel: 44 1223 336405*

[b] *Dept. of Chemistry, Joseph Black Building, University of Glasgow, Glasgow, UK G12 8QQ*

[c] *Institute of Biomedical and Life Sciences, Division of Biochemistry and Molecular Biology, University of Glasgow, Glasgow, UK G12 8QQ*

Received 23rd May 2005, Accepted 19th July 2005
First published as an Advance Article on the web 1st August 2005

Selective inhibitors of type II dehydroquinase were rationally designed to explore a second binding-pocket in the active-site. The molecular modelling, synthesis, inhibition studies and crystal structure determination are described.

The shikimate pathway is involved in the biosynthesis of aromatic amino acids and other key metabolites, and has been found in plants, bacteria, fungi and some parasites, but not in mammals.[1] It is a recognised target in the development of novel herbicides and antimicrobial agents. The third step in this pathway is the dehydration of 3-dehydroquinate (**1**) to 3-dehydroshikimate (**2**) (Scheme 1), catalysed by dehydroquinase (EC 4.2.1.10, 3-dehydroquinate dehydratase).[2] This step is also part of the quinate pathway in fungi.[1] There are two types of dehydroquinase, which are structurally distinct and catalyse the same transformation by different mechanisms.[3,4] Type I dehydroquinases are dimeric proteins with a 26–28 kDa subunit and catalyse the *syn* dehydration of **1** through the formation of a Schiff base.[2,5] Type II dehydroquinases are dodecamers of subunit 12–18 kDa and catalyse the *anti* elimination of water *via* an enolate intermediate.[6] Since only type II dehydroquinases are present in important pathogens such as *Mycobacterium tuberculosis*[7] and *Helicobacter pylori*,[8] specific inhibitors of these enzymes have therapeutic potential.

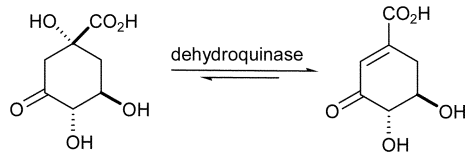

1 **2**

Scheme 1 The reaction catalysed by dehydroquinase.

The first generation of mechanism-based inhibitors was based on mimicking the flattened enolate intermediate.[9] The anhydro compound **3** had a K_I of 30 μM against *Streptomyces coelicolor* type II dehydroquinase and was significantly more potent than the reduced analogue **4** (K_I = 600 μM). A crystal structure of *S. coelicolor* type II dehydroquinase with **3** bound in the active site revealed a second binding-pocket, which was occupied by a glycerol molecule (PDB code: 1GU1) (Fig. 1a).[10] Subsequently, bifunctional compounds with a quinate core and side-chains from C-3 to reach into this second binding site were designed. The primary alcohol **5** was the most potent of these compounds but had a modest K_I of 180 μM against *S. coelicolor* type II dehydroquinase.[11] In order to derive more benefit from this second binding site, a range of substituted benzyl groups were attached to the C-1 and C-4 hydroxyl groups of **3**.[12] Molecular docking suggested that the substituted benzyl groups would bind at the "glycerol" pocket, and the most potent compound (**6**, K_I = 8 μM) included a 2-nitrobenzyl substituent. We have now combined these strategies and designed compounds **7–9** to have pendant aromatic groups attached to side chains attached to C-3 of the quinate core.

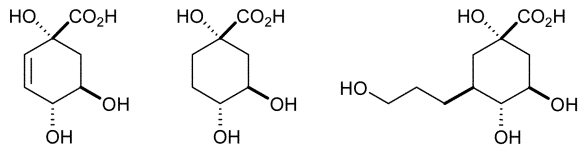

3

4

5

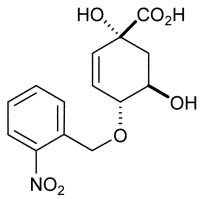

6

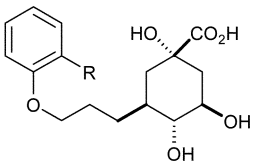

7 R = H
8 R = NO_2
9 R = CO_2H

Molecular docking with the program GOLD (version 2.1)[13] was used to predict the binding modes of **7–9**. These ligands were docked to the type II dehydroquinase structure (1GU1), which was prepared using Sybyl6.5.[14] The result from **7** is shown in Fig. 1a, compared with the position of **3** in the crystal structure. Both **8** and **9** docked in the same orientation (see ESI†). The quinate ring docks in a similar position to **3**, and the side-chain reaches to the second binding-pocket, which appears to be large enough to accommodate the phenyl ring. The modelling suggests ring-stacking between the ligands' phenyl group and the side-chain of Tyr-28, and a possible interaction of any *ortho*-substituent with Arg-23.

The target compounds (**7–9**) were synthesised from quinic acid (**10**) according to the method outlined in Scheme 2. The intermediate **11** was prepared in three steps using known methods[16] and the free hydroxyl was acetylated with acetic anhydride in pyridine in 96% yield to give **12**. The anti-Markovnikov bromination of the allyl side-chain to form **13** was achieved in high yield (97%) by bubbling HBr through a solution of **12** in carbon tetrachloride in the presence of catalytic AIBN. This terminal bromide was the key branch-point in the synthetic strategy. It was reacted with phenol, 2-nitrophenol and methyl 2-hydroxybenzoate, in the presence of sodium hydride and potassium iodide (catalytic), and heated

† Electronic supplementary information (ESI) available: experimental details. See http://dx.doi.org/10.1039/b507156a

DOI: 10.1039/b507156a

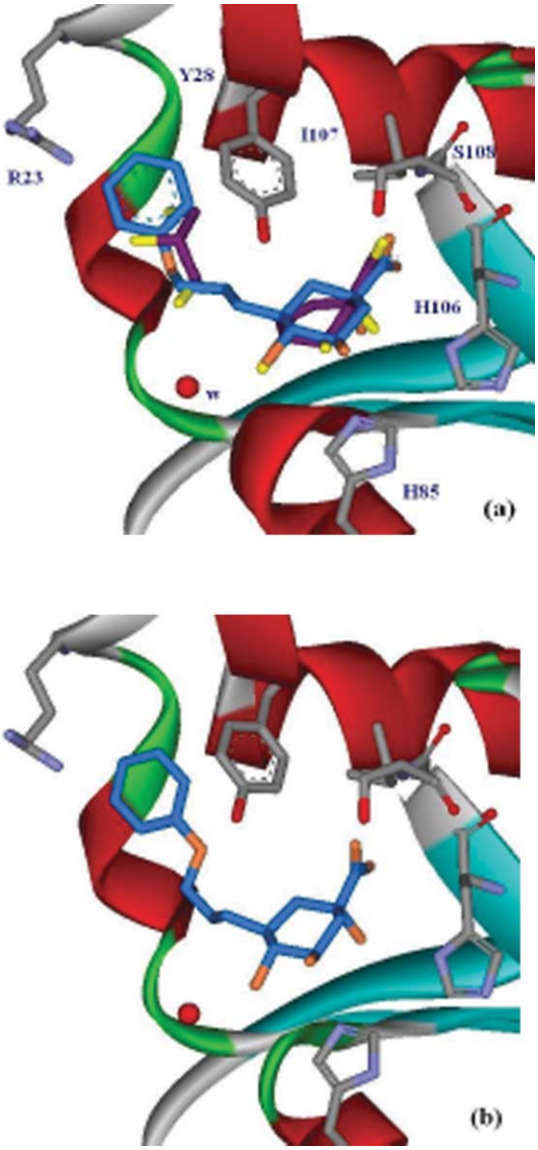

Fig. 1 [15] (a) Active-site view of the *S. coelicolor* type II dehydroquinase crystal structure with **3** and glycerol (purple) bound (PDB code: 1GU1[10]). Comparison between the position of **3** and the docking result of **7** (blue); (b) active-site view of the *S. coelicolor* type II dehydroquinase crystal structure with **7** (blue) bound (PDB code: 2BT4).

to reflux in acetonitrile to give **14** (69% yield), **15** (11%) and **16** (23%), respectively. The yields reflect the nucleophilicity of the phenols (PhOH > 2-MeO_2CPhOH > 2-O_2NPhOH). This strategy potentially allows the attachment of a wide range of nucleophiles, such as other alcohols, amines or thiols, to the propyl side-chain of these quinate analogues. Full deprotection of all compounds (**14–16**) was achieved by treatment with sodium hydroxide in a MeCN–H_2O (1 : 1) solution at room-temperature and the products **7–9** were obtained as a 1 : 1 mixture with benzoate. The pure ammonium salts of the target compounds were obtained after HPLC purification through a C-18 reverse-phase column eluting with a gradient of H_2O–MeCN and treatment with ammonium bicarbonate.

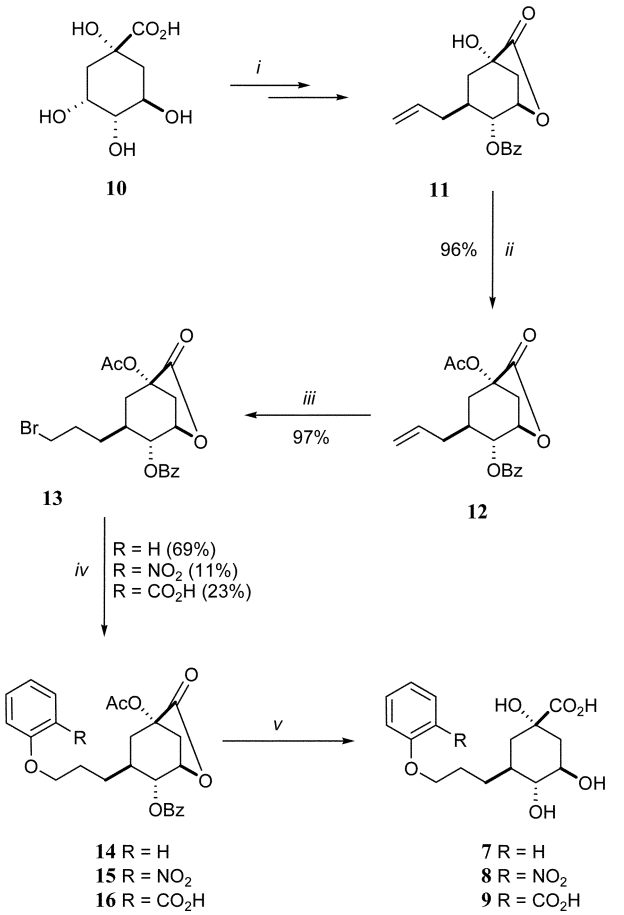

Scheme 2 *Reagents and conditions*: (i) ref. 16; (ii) Ac_2O, pyridine, RT; (iii) HBr, CCl_4, RT; (iv) 2-RPhOH, NaH, NaI, MeCN, Δ; (v) 1. NaOH, H_2O–MeCN (1 : 1), 2. HPLC purification (reverse phase, H_2O–MeCN gradient).

The analogues **7–9** were tested for inhibition against type I (*Salmonella typhi*) and type II (*S. coelicolor*) dehydroquinases by monitoring the formation of product at 232 nm.[17] The results are shown in Table 1. None of the compounds showed any inhibition against the type I enzyme within the sensitivity of the assay, which is consistent with all the results obtained on C-3 substituted quinate analogues. However all three compounds showed competitive reversible inhibition against type II dehydroquinase. Compound **7** is the best inhibitor of the *S. coelicolor* type II enzyme, with a K_I of 33 μM. This inhibitor has a similar K_I to **3** and is 20 times more potent than the reduced analogue **4**, and 6 times more potent than **5**, which emphasises the importance of the benzyl ring. The analogues with a 2-substituted phenyl ring, **8** and **9**, had K_I values of 84 and 220 μM respectively, which is in contrast with the positive effect of the 2-nitro group on **6**. These results show a trend where increase of hydrophilicity at the 2-position in the ring is unfavourable, suggesting that there is no positive interaction with the Arg-23 side-chain.

The best inhibitor of this set, **7**, was crystallised with *S. coelicolor* type II dehydroquinase and the crystal structure

Table 1 Inhibition constants (μM) for type I (*S. typhi*) and type II (*S. coelicolor*) dehydroquinases

Compounds	**3**	**4**	**5**	**6**	**7**	**8**	**9**
Type I (*S. typhi*)[a]	3000 ± 1000[b]	4500 ± 500[b]	>20 000[c]	—	>20 000	>20 000	>20 000
Type II (*S. coelicolor*)[a]	30 ± 10[b]	600 ± 200[b]	180 ± 20[c]	8 ± 2[d]	33 ± 5.4	84 ± 13	220 ± 50

[a] K_M values of 16 μM (*S. typhi* type I dehydroquinase) and 250 μM (*S. coelicolor* type II dehydroquinase) were obtained, using the standard assay.[17] [b] Ref. 9. [c] Ref. 11. [d] Ref. 12.

shows the compound binding at the active-site (Fig. 1b). The quinate ring is in a similar position as **3** in the main binding-pocket with the exception of C-2, which in the absence of a double bond is moved by 0.85 Å, the quinate ring adopting a full chair conformation. The carboxyl interactions with the backbond amides of Ile-107 and Ser-108 are essentially the same, while the H-bond from the hydroxyl group at C-1 with the side chain of His-106 is longer (0.1 Å). The quinate ring of **7** is moved away from the protein by ~0.3 Å and as a result H-bonding distances between the hydroxyl groups at C-4 and C-5 with His-85 and Arg-117 (not shown) are slightly changed (by +0.1 and −0.2 Å, respectively). This movement is accompanied by a 0.5 Å movement in the water conserved in all *S. coelicolor* type II dehydroquinase structures and implicated in the mechanism.[10] This water movement is caused by the side-chain at C-3 extending into the "glycerol" binding-pocket, where there is ring-stacking between the benzyl ring and Tyr-28. In addition, the benzene ring displaces two water molecules and effects the position of a third buried water.

Despite some disruption to the structure, the side-chain at C-3, which extends into the "glycerol" binding-pocket must account for the increased potency of **7**. The position of **7** in the active site agrees well with the binding position predicted by molecular docking (Fig. 1a *vs.* 1b), validating the strategy and methods used in this project. Further optimisation of **7**, to reduce the unfavourable interactions identified from the crystal structure should lead to significantly more potent specific inhibitors of type II dehydroquinase than are currently available.

In summary, we have rationally designed a set of compounds to explore specific interactions at a second binding-pocket in the active site of type II dehydroquinase, achieving an increase in potency, with **7** in particular, and high selectivity. Structural information showed **7** in a position consistent with molecular docking experiments, and identified key interactions to optimise in future compounds.

Acknowledgements

We would like to thank Fundação para a Ciência e a Tecnologia for financial support.

References

1 C. Abell, in *Enzymology and Molecular Biology of the Shikimate Pathway; Comprehensive Natural Products Chemistry*, ed. U. Sankawa, Pergamon, Elsevier Science Ltd., Oxford, 1999, pp. 573–607.
2 C. Kleanthous, R. Deka, K. Davis, S. M. Kelly, A. Cooper, S. E. Harding, N. C. Price, A. R. Hawkins and J. R. Coggins, *Biochem. J.*, 1992, **282**, 687–695.
3 V. B. Patel, M. Schweizer, C. C. Dyskstra, S. R. Kushner and N. H. Giles, *Proc. Natl. Acad. Sci. USA*, 1981, **78**, 5783–5787.
4 D. G. Gourley, A. K. Shrive, I. Polikarpov, T. Krell, J. R. Coggins, A. R. Hawkins, N. W. Isaacs and L. Sawyer, *Nat. Struct. Biol.*, 1999, **6**, 521–525.
5 (*a*) C. Kleanthous, M. Reilly, A. Cooper, S. Kelly, N. C. Price and J. R. Coggins, *J. Biol. Chem.*, 1991, **266**, 10893–10898; (*b*) R. K. Deka, C. Kleanthous and J. R. Coggins, *J. Biol. Chem.*, 1992, **267**, 22237–22242; (*c*) A. P. Leech, R. James, J. R. Coggins and C. Kleanthous, *J. Biol. Chem.*, 1995, **270**, 25827–25836.
6 (*a*) J. Harris, C. Kleanthous, J. R. Coggins, A. R. Hawkins and C. Abell, *J. Chem. Soc., Chem. Commun.*, 1993, **270**, 1080–1081; (*b*) A. Shneier, J. Harris, C. Kleanthous, J. R. Coggins, A. R. Hawkins and C. Abell, *Bioorg. Med. Chem. Lett.*, 1993, **3**, 1399–1402; (*c*) J. M. Harris, C. Gonzalez-Bello, C. Kleanthous, A. R. Hawkins, J. R. Coggins and C. Abell, *Biochem. J.*, 1996, **319**, 333–336.
7 T. Garbe, S. Servos, A. Hawkins, G. Dimitriadis, D. Young, G. Dougan and I. Charles, *Mol. Gen. Genet.*, 1991, **228**, 385–392.
8 J. R. Bottomley, C. L. Clayton, P. A. Chalk and C. Kleanthous, *Biochem. J.*, 1996, **319**, 559–565.
9 M. Frederickson, E. J. Parker, A. R. Hawkins, J. R. Coggins and C. Abell, *J. Org. Chem.*, 1999, **64**, 2612–2613.
10 A. W. Roszak, D. A. Robinson, T. Krell, I. S. Hunter, M. Fredrickson, C. Abell, J. R. Coggins and A. Lapthorn, *Structure*, 2002, **10**, 493–503.
11 M. D. Toscano, M. Frederickson, D. P. Evans, J. R. Coggins, C. Abell and C. González-Bello, *Org. Biomol. Chem.*, 2003, **1**, 2075–2083.
12 C. González-Bello, E. Lence, M. D. Toscano, L. Castedo, J. R. Coggins and C. Abell, *J. Med. Chem.*, 2003, **46**, 5735–5744.
13 (*a*) G. Jones, P. Willet and R. C. Glen, *J. Mol. Biol.*, 1995, **245**, 43–53; (*b*) G. Jones, P. Willet, R. C. Glen, A. R. Leach and R. Taylor, *J. Mol. Biol.*, 1997, **267**, 727–748.
14 SYBYL. 6.5. 1699 South Hanley Road, St. Louis, Missouri, 63144, USA: Tripos Inc.
15 WebLab ViewerPro4.0. 9685 Scranton Road, San Diego, CA 92121, USA: Accelrys Inc.
16 T. Widlanski, S. L. Bender and J. R. Knowles, *Biochemistry*, 1989, **28**, 7572–7582.
17 UV assay monitored the formation of 3-dehydroshikimate at 234 nm using black-walled quartz cuvettes. All assays were done in 1 ml reaction volumes, at 25 °C and pH 7.0 (50 mM potassium phosphate buffer for type I dehydroquinase; 50 mM Tris-HCl buffer for type II dehydroquinase).